Optica Applicata, Vol. XLI, No. 3, 2011

Light scattering models of white blood cells and back-scattering distribution analysis of them

YA-WEI WANG, MIN BU, XUE-FU SHANG, QU-WEI YUE

The School of Science, Jiangsu University, Zhenjiang, Jiangsu, China 212013

Corresponding authors: Y.-W. Wang – jszjwyw@yahoo.com.cn, M. Bu – bumin@ujs.edu.cn, X.-F. Shang – shangxuefu@gmail.com, Q.-W. Yue – floral041@yahoo.com.cn

Focusing on the light scattering technique and its application in cell identification, the analysis of the morphological structures of the WBCs (white blood cells) has been made, and the light scattering models of five types of the WBCs have been built. Based on the light scattering theory and applying numerical simulation techniques to a systematic study of the back-scattering intensity distribution of five types of the WBCs, some significant effects made by the internal and external morphological structures of the WBCs and the changes of their refractive index to their back-scattering distribution and certain relations between them have been found. Thus, the back-scattering theory and its application have been expanded, and it is very useful to improve the technique of cell identification.

Keywords: cell identification, WBC (leukocyte), analysis of scattering, back-scattering.

1. Introduction

The classification and detection of the biological cells have a very important application in many fields, such as life science, medical diagnosis, *etc*. Since the theory of light scattering was used in cell detection, applications of the various optical detection technologies to the study of the components and morphological distribution of biological cells have become one of the hot research issues. WBCs, with the various types, are divided into five types which include neutrophils, eosinophils, basophils, monocytes and lymphocytes. According to the optical scattering detection theory on cells: light scattering occurs when the beam is incident on a blood cell. Light scattering of blood cells includes diffraction, refraction, reflection and absorption. Different cells have their own biochemical structures and refractive index and contain substances of different shape and volume. Therefore, the light scattering chromatogram of a blood cell is in connection with not only the cell's volume, but also its shape, orientation, internal structure and the refractive index distribution.

SCHMITT and KUMAR [1] proved that different refractive indices and their changes will cause the variations in scattering. VIDEEN *et al.* [2], ENEJDER *et al.* [3], and

KAHNERT *et al.* [4] made theoretical and experimental studies on light scattering from particles with different shapes; FLYNN *et al.* [5], BARTLETT *et al.* [6] made research into the methods of light scattering detection; PAWLOWSKI *et al.* [7], LUGOVTSOV *et al.* [8], JUN Q. LU *et al.* [9], TANEV *et al.* [10], DENSMORE *et al.* [11] made a lot of original studies concerning models of cell deformation, ellipsoid orientation, and numerical computation. Because the application of light scattering technology to the biological cell detection is promising, our group has been studying the character of light scattering from biological cells since the late twentieth century, acquiring a number of important conclusions about the forward light scattering characteristic distributions of cells [12–14]. However, due to its unique characteristics, much research work about the back-scattering is still to be done and the understanding of it is not deep enough, as a result of which the light scattering technology for cells finds little substantial application. For this reason, we have established five types of physical models of leukocyte by analyzing the optical characteristics of the WBCs, making a systematic study of the backward light scattering distributions of the five types of WBCs, which is based on the light scattering theory and the method of applying numerical simulation computing techniques, and obtained some important conclusions which provide a strong theoretical and technical support for improving the optical measurement technology of leukocyte and for the application of the backward light scattering technology.

2. Five types of WBCs and the light scattering models

In general, WBCs, with the diameter of 7–20 μm, are cells of spherical nucleus and can be divided into two types: granulocytes and granularless leukocytes; according to the chromophil character of the specific granule, granulocytes can be classified into neutrophil, eosinophil and basophil, and granularless leukocytes can be categorized into lymphocytes and monocytes. Their size from small to large is: lymphocyte < basophil < neutrophil < eosinophil < monocyte. Among them,

1) Neutrophils, with their spherical structures and the diameter of 10–12 μm, have the largest number in white blood cells and contain small, round or oval particles with the diameter of 0.6–0.7 μm. The nucleus of neutrophil is rod-shaped or lobulated and generally can be divided into 2 to 5 pieces. The shapes of the nuclei are various. Some are sausage-shaped and others are connected lobulated.

2) The diameter of a eosinophil is 10–15 μm. The cell is spherically shaped and its nucleus often has two pieces. The cytoplasm is filled with coarse (diameter of 0.5–1.0 μm), well-distributed and slightly refracting granules which are generally oval in shape.

3) Basophils, with the diameter of 10–12 μm, are the least number of the leukocytes. The cell is spherically shaped and its nucleus is lobulated, S-shaped or irregular, lightly colored and unclearly outlined.

4) The monocyte with the diameter of 14–20 μm is spherical or oval in shape. The cytoplasm is abundant and contains many small particles; the shapes of the nuclei

are various, such as kidney-shaped, horseshoe-shaped, oval or irregular, and their color is lighter.

5) Lymphocytes are different in size and shaped as round or oval. The nucleus of a lymphocyte is round or oval in shape. The diameter of a small lymphocyte is 6–8 μm; 9–12 μm in a medium one; and 13–20 μm in a large one. The lymphocytes in the blood are mostly the small ones. The nucleus is round-shaped and a shallow concavity often appears on one side of it. The chromatin with a small amount of cytoplasm is densely shaped as lumpy masses and forms a narrow band around the nucleus.

From the morphological structures of the five types of WBCs given above, it can be seen that the sphericity and ellipsoid are two main shapes of both the external form and internal karyomorphology. For this reason, we have built up some spherical models to denote the external forms of the neutrophil, eosinophil and basophil; spherical and ellipsoid-based models of the monocyte and lymphocyte; and global, ellipsoidal nuclei or the ones with deformable morphological factors for both regular and irregular internal structures of the leukocytes. And we use the changes in their morphological structures to symbolically express the differences between the nucleus and the soma.

For a general model of dielectric sphere, Lorenz and Mie obtained the exact solution for the scattering of electromagnetic wave by a sphere. VAN DE HULST presented the results of two amplitude functions [15]:

$$S_1(\alpha, m, \theta) = \sum_{n=1}^{\infty} \frac{2n+1}{n(n+1)} \left[a_n(\alpha, m)\pi_n(\cos\theta) + b_n(\alpha, m)\tau_n(\cos\theta) \right] \tag{1}$$

$$S_2(\alpha, m, \theta) = \sum_{n=1}^{\infty} \frac{2n+1}{n(n+1)} \left[a_n(\alpha, m)\tau_n(\cos\theta) + b_n(\alpha, m)\pi_n(\cos\theta) \right] \tag{2}$$

where the Legendre functions π_n and τ_n are the angular coefficients connected with the scattering angle; a_n and b_n are Mie scattering coefficients; m is the relative refractive index and it is defined as the quotient of the refractive index of the particle m_2 divided by that of the medium m_1. $\alpha = 2\pi a/\lambda$ is a dimensionless size parameter, where a is the radius of spherical particle and λ is the wavelength of the incident light. The subscripts 1 and 2 refer to the perpendicular and parallel incidence of plane-polarized light to the scattering plane, respectively.

If $\alpha \gg 1$, Van de Hulst showed that the expansions in Eqs. (1) and (2) may be truncated at $n + 0.5 \approx \alpha$ and the remaining finite sum is separated into two parts. One is independent of the nature of the particle. It describes the diffracted light field component:

$$S_{D1}(\alpha, \theta) = S_{D2}(\alpha, \theta) = \alpha^2 \frac{J_1(\alpha \sin\theta)}{\alpha \sin\theta} \tag{3}$$

where J_1 is the 1st-order Bessel function. This is identical to the Fraunhofer diffraction pattern calculated for an opaque disk by using the scalar theory. The other is dependent on the nature of the particle. UNGUT *et al.* [16] explained the light scattering of spherical

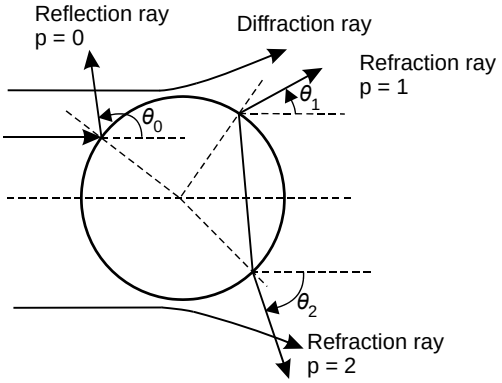

Fig. 1. Theoretical model for geometrical optics approximation.

particles by using the geometrical-optics formalism and presented the results of amplitude functions for reflected and refracted light fields:

$$S_{1,2}(\theta) = \sum_{p,q} \alpha E_{1,2} \left[\frac{\sin(2\theta_i)}{\sin(\theta)\left|\frac{\mathrm{d}\theta_p}{\mathrm{d}\theta_i}\right|} \right]^{0.5} \exp\left[i\delta + \frac{i\pi}{2}\left(p + 1 - \frac{1}{2}q - \frac{1}{2}s - 2l\right) \right] \tag{4}$$

where p is the number of internal reflections. Figure 1 shows that, for $p = 0$, the ray is externally reflected; for $p = 1$, the ray is refracted and leaves the particle without any internal reflection; and for $p > 1$, the ray is internally reflected. θ_p is a deflecting angle and is defined as: $\theta_p = 2p\theta_r - 2\theta_i - p\pi + \pi$, where θ_i is the angle of incidence and θ_r is the angle of refraction, and they are related to each other by Snell's law. The relative refractive index $m = \sin\theta_i / \sin\theta_r$. $\theta_p = q\theta - l2\pi$ is related to the scattering angle θ; $q = 1$ indicates that the incident ray hits the scattering particle on the upper hemisphere and $q = -1$ for the lower hemisphere; l is an integer which must be chosen so that the scattering angle θ in the range can be between 0 and π; $s = -1$ for $m > 1$ and $s = 1$ for $m < 1$. $E_{1,2}$ is defined as:

$$\begin{cases} E_{1,2} = r_{1,2} & p = 0 \\ E_{1,2} = (1 - r_{1,2}^2)(-r_{1,2}^2)^{p-1} & p > 0 \end{cases} \tag{5}$$

$$r_1 = \frac{\cos\theta_i - m\cos\theta_r}{\cos\theta_i + m\cos\theta_r} \tag{6}$$

$$r_2 = \frac{m\cos\theta_i - \cos\theta_r}{m\cos\theta_i + \cos\theta_r} \tag{7}$$

where r_1 and r_2 are Fresnel reflection coefficients. The phase difference δ is given by

$$\delta = 2\alpha(\cos\theta_i - pm\cos\theta_r) \tag{8}$$

3. Distributions of back-scattering for various models

3.1. Single-sphere model

According to the diffraction theory, the diffractive effect appears only in the forward scattering direction; and in the single-sphere back-scattering simulation, only the reflective and refractive effects are considered in the back-scattering direction. So, the theory discussed above can be similar to

$$S_j(\theta) = \sum_{p=0}^{\infty} S(\alpha, m, \theta)$$

$$i(\theta) = \frac{S_1 S_1^* + S_2 S_2^*}{2}$$

$$\theta \subset [0.5\pi, \pi]$$

Supposing that the diameter of a cell is 9.17 μm, then $\alpha = 90.9$. Adjusting the refractive index of suspension to get close to the relative one of cell liquid, where $m = 1.0007 \sim 1$, the numerical simulation result is shown as Fig. 2. It can be seen that the backward scattering intensity aperiodically oscillates as the angle changes and that the change of the light intensity within certain angle is not drastic.

3.2. Concentric sphere model

The external and internal spheroids represent a cell and the nucleus of that cell, respectively. Similarly, based on the diffraction theory, only influences of reflection

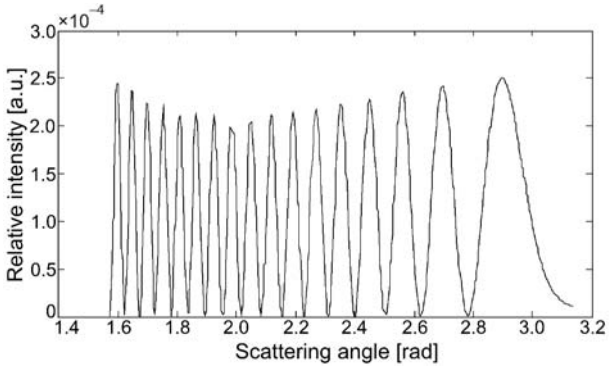

Fig. 2. Angular distribution of back-scattered light intensity of a single-sphere model.

and refraction from the internal and external spheroids are considered in the back--scattering simulation. Adjusting the refractive index of suspension to get close to that of cytoplasm makes the light that irradiates to the nucleus still parallel light. The reflection between the external spheroid and the nucleus will increase the number of the reflected light while the light intensity will decrease drastically. So, for the external spheroid, those contributions made by the light ($p > 1$) to scattering intensity can be ignored. Put $p = 0$, $q = +1$, $l = 0$, $s = -1$ into formula (4), then

$$S_{01} = \frac{\sqrt{2}}{2}\alpha \frac{\sin\left(\frac{\theta}{2}\right) - \sqrt{m^2 - \cos^2\left(\frac{\theta}{2}\right)}}{\sin\left(\frac{\theta}{2}\right) + \sqrt{m^2 - \cos^2\left(\frac{\theta}{2}\right)}} \exp\left\{ i\left[2\alpha\sin\left(\frac{\theta}{2}\right) + \frac{\pi}{2}\right]\right\} \tag{9a}$$

$$S_{02} = \frac{\sqrt{2}}{2}\alpha \frac{m^2\sin\left(\frac{\theta}{2}\right) - \sqrt{m^2 - \cos^2\left(\frac{\theta}{2}\right)}}{m^2\sin\left(\frac{\theta}{2}\right) + \sqrt{m^2 - \cos^2\left(\frac{\theta}{2}\right)}} \exp\left\{ i\left[2\alpha\sin\left(\frac{\theta}{2}\right) + \frac{\pi}{2}\right]\right\} \tag{9b}$$

Defining nucleocytoplasmic ratio as $t = r/R$, r is the radius of nucleus and R is the radius of the cell, m' is the refractive index of nucleus relative to that of cytoplasm. Taking the WBC as an example, the diameter of the nucleus is chosen as 6.66 μm and its refractive index is set to be 1.440 while the diameter of the cell is selected as 9.17 μm and the refractive index is 1.358. Adjusting the refractive index of normal saline to the point of 1.359 and the wavelength of He-Ne laser of 20 mW to 633 nm, then $\alpha = 90.9$, $m = 1.0007 \sim 1$, $t = 0.71$, $m' = 1.06$, the result of simulation calculation is shown as Fig. 3.

In addition, for $t = 0.11$, $t = 0.31$, $t = 0.51$, and $t = 0.91$, the simulation results of light intensity distributions are shown in Fig. 4. It can be seen from the simulation

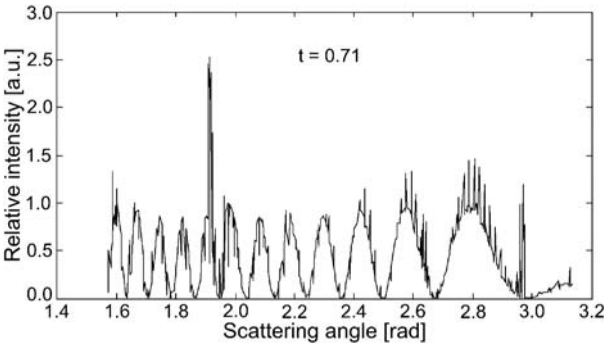

Fig. 3. Angular distribution of back-scattered light intensity of a concentric sphere model when $t = 0.71$.

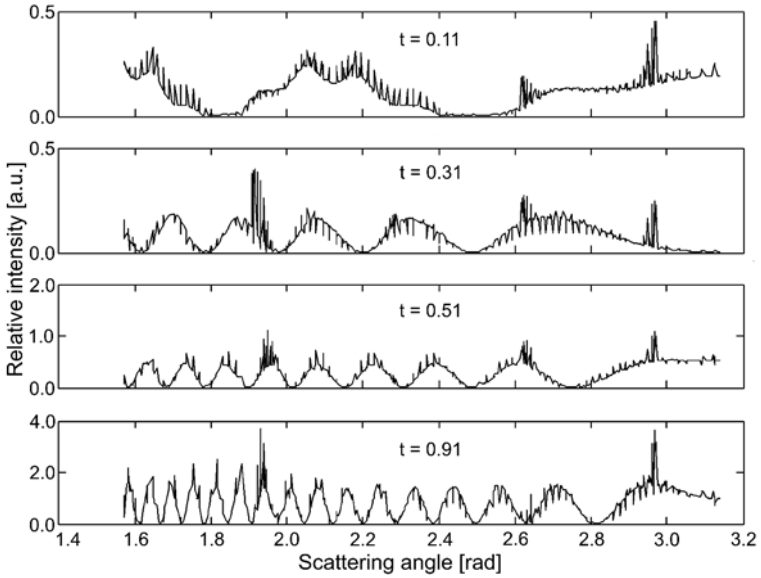

Fig. 4. Angular distribution of back-scattered light intensity of a concentric sphere model for different values of *t*.

results that back-scattering makes two significant changes as *t* increases. One is the increase of the scattering light intensity and the other is the decrease of the oscillation cycle.

3.3. Eccentric sphere model

If the hearts of the internal and external spheres do not overlap, the concentric sphere will be an eccentric sphere. By adopting parallel light incidence and studying light intensity distribution which is relative to scattering angle and from geometric scattering theory, it can be concluded that the back-scattering light in such a model is the same as that of the concentric sphere model while the forward scattering light makes some slight changes, and it does not matter whether the angle between the line which connects two sphere centers and the ingoing parallel light is equal to zero or not.

3.4. Ellipsoid and concentric ellipsoid model

Based on the Rayleigh–Debye–Gans approximation, a simulation of two concentric rotating ellipsoids was made to a true nucleated cell and the study was concentrated only on single-scattering and elastic light-scattering. Our group obtained the following mathematical expressions of the amplitude function for the scattered light [17]:

$$\left.\begin{matrix} S_1(\theta) \\ S_2(\theta) \end{matrix}\right\} = i k_0^3 \alpha(r) P(\theta) \left\{\begin{matrix} 1 \\ \cos\theta \end{matrix}\right. \tag{10}$$

$$P(\theta) = \eta\int_0^{\pi} \mathrm{d}\varphi \int_0^{2\pi} \mathrm{d}\rho \int_0^{a} \alpha_a' \left| m_a^2 - 1 \right| e^{i2k_0 m_a r\sqrt{1+(\eta^2-1)\cos^2(\rho)\sin^2(\varphi)}\sin\left(\frac{\theta}{2}\right)} r^2 \sin(\varphi)\mathrm{d}r +$$

$$+ \eta\int_0^{\pi} \mathrm{d}\varphi \int_0^{2\pi} \mathrm{d}\rho \int_a^{b} \alpha_b' \left| m_b^2 - 1 \right| e^{i2k_0 m_b r\sqrt{1+(\eta^2-1)\cos^2(\rho)\sin^2(\varphi)}\sin\left(\frac{\theta}{2}\right)} r^2 \sin(\varphi)\mathrm{d}r \tag{11}$$

where $P(\theta)$ is a modality factor which is related to the volume, shape and refractive index of a cell, $\alpha(r)$ refers to the volume polarizability, η is a body factor and is defined as the ratio of the major and minor semi-axis of rotational symmetry ellipsoid, a and b are the minor semi-axis of the nucleus and the cell, respectively. Selecting $a = 2$ μm, $b = 5$ μm, $m_a = 1.10$, $m_a = 1.08$ and the body factors as 1.3, 2 and 5, respectively, the amplitude distribution can be obtained by simulating after numerical computation and shown in Fig. 5. The figure gives a comparison of different distributing graphs under three situations. Figure 5 shows that the scattering intensity vibrates within 0–π degrees; the forward scattering intensity is stronger than the backward one which responses to Mie scattering theory; the oscillation cycles of back-scattering and side-scattering are accelerating with the increase of cells' body factor.

Under the condition of non-axial incidence, selecting the angles of incidence β as 0°, 30°, 60°, respectively, to discuss each situation, the amplitude distribution can be obtained by simulation. It is shown in Fig. 6 after numerical computation. The figure demonstrates that the distribution pattern of scattered light amplitude almost does not change under the three incidence conditions; but, as the angle of incidence enlarges, the scattering amplitude will increase.

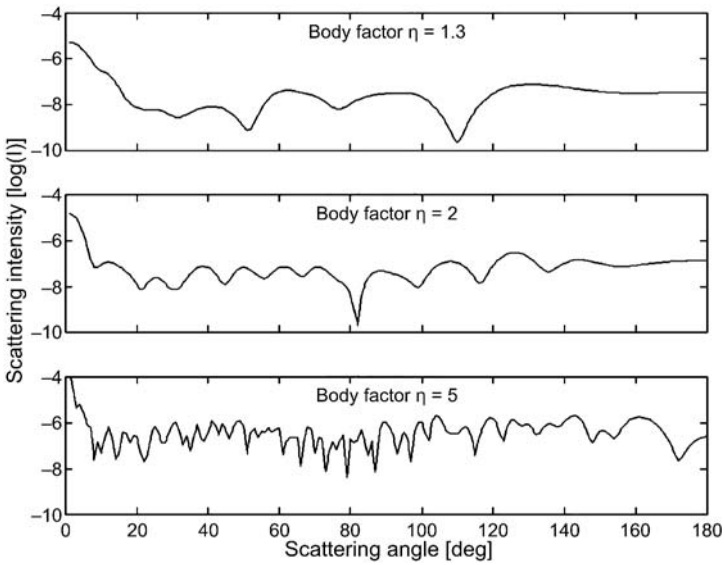

Fig. 5. Logarithm distribution of scattering intensity for different body factors.

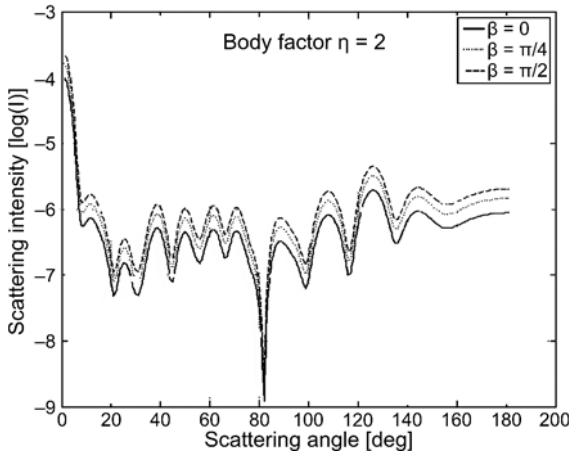

Fig. 6. Logarithm distribution of scattering intensity for different angles of incidence.

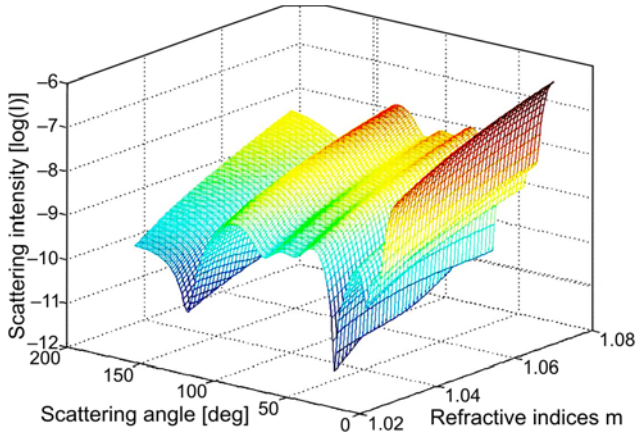

Fig. 7. Scattering intensity distribution for the continuously varying refractive index.

The value of *m* in general pathological condition is easy to exceed the normal scope, and the change of refractive index will have a greater influence on scattered light. In the following numerical simulation, making "*m*" changeable around the normal value (1.03–1.07), and the amplitude distribution can be obtained and shown in Fig. 7. It can be seen from Fig. 7 that there is little variety in the scattering distribution of a cell compared with another one of the same shape and the scattering distribution vibrates within 0–π degrees; the scattering intensity enhances as the refractive index increases.

3.5. Multinucleated model

It can be derived from the theory given above that, if a cell or the nuclei of a cell can be seen as a sphere, adjusting the refractive index of the suspension equally to that of the cytosol, the angular distribution of scattering light intensity will be the same as

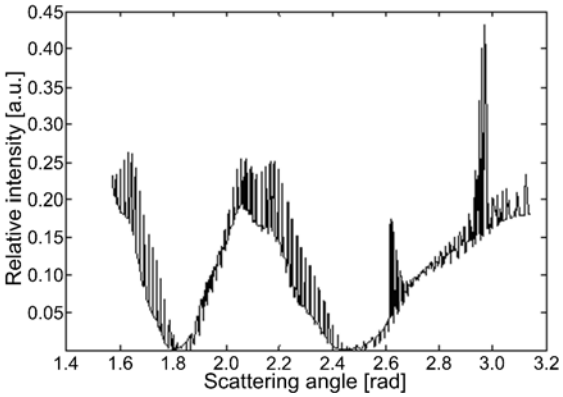

Fig. 8. Back-scattering intensity distribution for trinucleated cell model.

the incoherent superposition of the scattering light intensity from each nucleus which stands alone in the center of the sphere and the one from the external spherical surface of the cell.

In such case, it provides a possibility to solve the problems that there are mitochondrions in the pleocaryocyte and cytosol. Supposing that all nuclei are the same in size and refractive index, $\alpha = 90.9$, $m = 1.0007 \sim 1$, $t = 0.11$, $m' = 1.06$ the back--scattering of the trinucleated cell is simulated, and the result is shown in Fig. 8. By comparing Fig. 8 with Fig. 4, it can be seen that the scattering distribution is similar to that of the monocyte with $t = 0.31$; the concussive shape of scattering distribution is similar to the case of monocyte with $t = 0.11$. Moreover, it can be seen that the scattering intensity of it is related to the total volume of inner nuclei and the chondriosome; and the concussive shape reflects the size of individual nucleus or chondriosome.

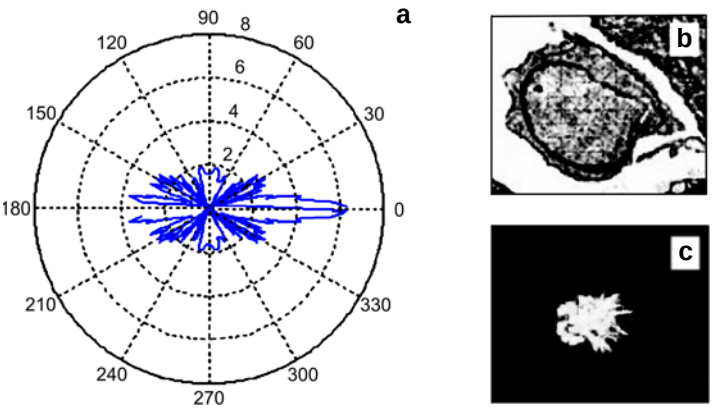

Fig. 9. Relative intensity distribution by GOA (**a**). A375 cell (**b**). Relative intensity distribution obtained in the experiment (**c**).

4. Experimental verification for such theoretical methods

The geometrical-optics approximation is also applicable to other spherical nuclear cell. We simulate a malignant melanoma cell (A375) and get the entire light intensity distribution of the cross-section. In order to facilitate the observation, the intensity is as shown in Fig. 9**a**. The Figure 9**c** shows the light intensity distribution of A375 in the suspension [18]. Simulation results not only correspond to the test results, but present the details which cannot be detected with the naked eye.

5. Conclusions

The models built in this article denote the five types of white blood cells in a better way and the theoretical methods are feasible. According to the research consequences, the following conclusions can be obtained by the analysis made above.

1) No matter what morphological structure of a cell is, that is, regardless of its category, the forward scattering intensity is stronger than the backward one which responses to Mie scattering theory. But a direct and simple relation between the back--scattering intensity and the volume and shape of a soma or nucleus has not been found yet.

2) For a model of any kind, the backward scattering intensity aperiodically oscillates as the angle changes and the change of light intensity within certain angle is not drastic. For a concentric sphere model, apart from the above characters, the back--scattering makes two significant changes as the nucleocytoplasmic ratio increases. One is the increase of scattering light intensity and the other is the decrease of oscillation cycle. This means that bigger nucleocytoplasmic volume makes back-scattering intensity stronger.

3) When the shape of a cell varies, the oscillation cycles of back-scattering and side-scattering are accelerating with the increase of cells' body factor. When the angle of incidence changes, the back-scattering distribution pattern of a cell almost does not change under different incidence conditions. But, as the angle of incidence enlarges, the scattering intensity will increase. There is little variety in the scattering distribution of a cell compared to another one of the same shape and the scattering distribution vibrates within 0–π degrees, and the scattering intensity enhances as the refractive index increases.

4) For a multinucleated model, that is, a model of a cell with more than one nucleus, its scattering distribution is similar to that of the monocyte and the concussive shape of scattering distribution is also similar to the case of monocyte. Moreover, it can be seen that the scattering intensity of it is related to the total volume of inner nuclei and that the concussive shape reflects the size of individual nucleus or chondriosome.

In summary, the back-scattering characteristics of a cell are specific, so they are necessary to be considered while studying the technology of detection and classifi-

cation to the five types of WBCs, and certain applications of the conclusions mentioned above to the cell classification and identification will greatly improve the accuracy of leukocyte classification and identification.

Acknowledgements – The authors gratefully acknowledge the support from the Natural Science Fund for colleges and universities in Jiangsu Province (No. 09KJA140001) and from the Key Laboratory of Quantum Optics of Jiangsu Province (Grant No. kjs0905).

References

[1] SCHMITT J.M., KUMAR G., *Turbulent nature of refractive-index variations in biological tissue*, Optics Letters **21**(16), 1996, pp. 1310–1312.

[2] VIDEEN G., PRABHU D.R., DAVIES M., GONZÁLEZ F., MORENO F., *Light scattering fluctuations of a soft spherical particle containing an inclusion*, Applied Optics **40**(24), 2001, pp. 4054–4057.

[3] ENEJDER A.M.K., SWARTLING J., ARUNA P., ANDERSSON-ENGELS S., *Influence of cell shape and aggregate formation on the optical properties of flowing whole blood*, Applied Optics **42**(7), 2003, pp. 1384–1394.

[4] KAHNERT F.M., STAMNES J.J., STAMNES K., *Can simple particle shapes be used to model scalar optical properties of an ensemble of wavelength-sized particles with complex shapes?*, Journal of the Optical Society of America A **19**(3), 2002, pp. 521–531.

[5] FLYNN R.A., BING SHAO, CHACHISVILIS M., OZKAN M., ESENER S.C., *Two-beam optical traps: Refractive index and size measurements of micro-scale objects*, Biomedical Microdevices **7**(2), 2005, pp. 93–97.

[6] BARTLETT M., HUANG G., LARCOM L., HUABEI JIANG, *Measurement of particle size distribution in mammalian cells in vitro by use of polarized light spectroscopy*, Applied Optics **43**(6), 2004, pp. 1296–1307.

[7] PAWLOWSKI P.H., BURZYNSKA B., ZIELENKIEWICZ P., *Theoretical model of reticulocyte to erythrocyte shape transformation*, Journal of Theoretical Biology **243**(1), 2006, pp. 24–38.

[8] LUGOVTSOV A.E., PRIEZZHEV A.V., NIKITIN S.YU., *Light scattering by arbitrarily oriented optically soft spheroidal particles: Calculation in geometric optics approximation*, Journal of Quantitative Spectroscopy and Radiative Transfer **106**(1–3), 2007, pp. 285–296.

[9] JUN Q. LU, PING YANG, XIN-HUA HU, *Simulations of light scattering from a biconcave red blood cell using the finite-difference time-domain method*, Journal of Biomedical Optics **10**(2), 2005, p. 024022.

[10] TANEV S., WENBO SUN, ZHANG R., RIDSDALE A., *Simulation tools solve light-scattering problems from biological cells*, Laser Focus World **40**(1), 2004, pp. 67–70.

[11] DENSMORE J.D., URBATSCH T.J., EVANS T.M., BUKSAS M.W., *A hybrid transport-diffusion method for Monte Carlo radiative-transfer simulations*, Journal of Computational Physics **222**(2), 2007, pp. 485–503.

[12] YAWEI WANG, GUANGCAI HAN, YING LIU, XIAONONG CHEN, WYROWSKI F., *The light scattering imitation of red blood cell under a double curve symmetrical model*, Chinese Journal of Lasers **34**(12), 2007, pp. 1676–1681.

[13] YAWEI WANG, BIN BU, QINGYI CUI, YUN HONG, DAJIAN WU, LAN CAI, *Researching on the distributing characters of light scattering from a nuclear-cell*, Chinese Journal of Lasers **33**(10), 2006, pp. 1434–1440.

[14] BIN DAI, XIANGDONG LUO, YAWEI WANG, *Multiple light scattering of non-spherical particles with elliptical cross section*, Acta Physica Sinica **58**(6), 2009, pp. 3864–3868.

[15] VAN DE HULST H.C., *Light Scattering by Small Particles*, Wiley, NewYork, 1957, pp. 201–208.
[16] UNGUT A., GREHAN G., GOUESBET G., *Comparisons between geometrical optics and Lorenz–Mie theory*, Applied Optics **20**(17), 1981, pp. 2911–2918.
[17] DAJIAN WU, YAWEI WANG, GUANGCAI HAN, *The model for elastic light scattering from nucleated cells*, Acta Optica Sinica **25**(12), 2005, pp. 1670–1675.
[18] WATSON D., HAGEN N., DIVER J., MARCHAND P., CHACHISVILIS M., *Elastic light scattering from single cells: orientational dynamics in optical trap*, Biophysical Journal **87**(2), 2004, pp. 1298–1306.

Received August 13, 2010
in revised form November 15, 2010